Available online at www.sciencedirect.com
ScienceDirect
Journal of Solid State Chemistry 180 (2007) 401–409
JOURNAL OF SOLID STATE CHEMISTRY
www.elsevier.com/locate/jssc

Structural phase transitions and crystal chemistry of the series $Ba_2LnB'O_6$ (Ln = lanthanide and B' = Nb^{5+} or Sb^{5+})

Paul J. Saines[a], Brendan J. Kennedy[a,*], Margaret M. Elcombe[b]

[a]School of Chemistry, The University of Sydney, Sydney, NSW 2006, Australia
[b]Bragg Institute, ANSTO, Private Mail Bag 1, Menai, NSW 2234, Australia

Received 7 September 2006; received in revised form 19 October 2006; accepted 20 October 2006
Available online 26 October 2006

Abstract

The structures of 28 compounds in the two series Ba_2LnSbO_6 and Ba_2LnNbO_6 have been examined using synchrotron X-ray and in selected cases neutron powder diffraction at, below and above ambient temperature. The antimonate series is found to undergo a sequence of phase transitions from monoclinic to rhombohedral to cubic symmetry with both decreasing ionic radii of the lanthanides and increasing temperature. Compounds in the series Ba_2LnNbO_6, on the other hand, feature an intermediate tetragonal structure instead of the rhombohedral structure exhibited by the antimonates. This difference in symmetry is thought to be caused by π-bonding in the niobates that is absent in the antimonates. The bonding environments of the cations in these compounds have also been examined with overbonding of the lanthanide and niobium cations being caused by the unusually large B-site cations.

Keywords: Perovskite; Crystal structure; Phase transitions; Metal oxides

1. Introduction

Double perovskites belonging to the series $Ba_2LnB'O_6$ (Ln = lanthanide and Y^{3+} and B' = Nb^{5+}, Ta^{5+}, Sb^{5+}) are of interest due to their potential use as substrates for high-T_c superconductors [1,2] and their likely high chemical compatibility with the structurally analogous, oxygen deficient double perovskites, $Ba_2LnSnO_{6-\delta}$; a series of interest for use as solid state electrolytes due to their high ionic conductivity [3,4]. Substitution of Nb^{5+}, Ta^{5+} or Sb^{5+} could provide a method of controlling the oxygen stoichiometry of these compounds, potentially minimizing the problems caused by reduction of $Ba_2LnSnO_{6-\delta}$ that is thought to be a consequence of the large level of oxygen vacancies in these compound [3].

In order to fully realize the potential of these compounds as substrates for high-T_c superconductors, or for use in solid oxide fuel cells, it is important to establish precise structures of $Ba_2LnB'O_6$ at ambient temperature and to understand how these structures evolve with changes in temperature. The nature of any phase transitions that these materials undergo has the potential to severely impact on their suitability for use in devices. First-order (discontinuous) phase transitions, in particular, can cause degradation in the performance of devices containing such materials due to delaminating and cracking.

Phase transitions in perovskites have long been of interest to solid-state chemists [5]. Previous studies by Fu and IJdo [6,7], using laboratory X-ray and medium-resolution neutron diffraction, reported that the structures in the series Ba_2LnSbO_6 change from $R\bar{3}$ rhombohedral (tilt system $a^-a^-a^-$) to $Fm\bar{3}m$ cubic ($a^0a^0a^0$) symmetry with decreasing size of the Ln^{3+} cation. Conversely the niobate series Ba_2LnNbO_6 exhibits the sequence: $I2/m$ monoclinic ($a^-a^-c^0$), $I4/m$ tetragonal ($a^0a^0c^-$) to $Fm\bar{3}m$ cubic symmetry. That the symmetry increases as the ionic radius of the lanthanide decreases is consistent with the increase of the tolerance factor t, $t = (r_{Ba} + r_O)/\sqrt{2}(\bar{r}_{(Ln,B')} + r_O)$ (r_{Ba} = radius of Ba^{2+}, r_O = radius of O^{2-} and $\bar{r}_{(Ln,B')}$ =

*Corresponding author. Fax: +61 2 9351 3329.
E-mail address: kennedyb@chem..usyd.edu.au (B.J. Kennedy).

0022-4596/$ - see front matter © 2006 Elsevier Inc. All rights reserved.
doi:10.1016/j.jssc.2006.10.017

average radius of the *Ln* and *B*′ cation in the perovskite structure), as the radii of the lanthanide decreases. An increase in the tolerance factor indicates that the volume of the BO_6 octahedron is better matched to the size of the AO_{12} polyhedron reducing the need for the octahedral tilting to accommodate this A-site cation. Since octahedral tilting is responsible for the lowering of the symmetry from cubic, the symmetry tends to increase as the B-type cation gets smaller.

Fu and IJdo [7] suggested that the niobate compounds adopt tetragonal symmetry, as opposed to the rhombohedral symmetry seen in the antimonates and other $Ba_2LnB'O_6$ (where $B' = Bi^{5+}$, Ir^{5+} and Ru^{5+}) oxides, as a result of covalent bonding [6,8–10]. They hypothesized that rhombohedral symmetry is favored when the *B*′ cation is more electronegative and hence the bonding is more covalent in nature whereas the tetragonal phase is preferred for less electronegative *B*′ cations such as Nb^{5+} where the bonding is more ionic. However, the recent report [11] that Ba_2NdMoO_6 has tetragonal $I4/m$ symmetry creates doubt about the cause of tetragonal symmetry in these compounds since Mo^{5+} has comparable electronegativity to Ir^{5+}, Ru^{5+} or Sb^{5+} [12]. Clearly another explanation is required and a re-examination of the structures in the series Ba_2LnNbO_6 and Ba_2LnSbO_6 is appropriate.

Further, there are conflicting reports whether the monoclinic space group in the Ba_2LnNbO_6 series is $P2_1/n$ ($a^+a^+c^-$), with a mixture or in- and out-of-phase tilts of the BO_6 octahedra, or $I2/m$ ($a^-a^-c^0$), that has only out-of-phase tilts [7,13]. Discriminating between these two monoclinic perovskite structures using powder X-ray diffraction can be difficult as the intensity of the *M*- and *X*-point reflections, diagnostic of the in-phase tilts is determined by the positions of the oxygen anions. Consequently the diagnostic *M*- and *X*-point reflections, are relatively weak in X-ray diffraction, particularly in the presence of very heavy elements such as the lanthanides. Neutron diffraction is much more sensitive to the positions of the oxygen anions than is X-ray diffraction for such oxides and as such is better suited to distinguishing between these two monoclinic space groups. The later work by Henmi et al. [13] described all members of the Ba_2LnNbO_6 series as featuring monoclinic symmetry in contrast with the various symmetries indicated by Fu and IJdo [7] highlighting the significant difficulty in correctly assigning the symmetry of double perovskites. Since the Ba_2LnNbO_6 and Ba_2LnSbO_6 compounds are of significant interest to solid-state chemists and material scientists confirmation of the structures of these compounds using a combination of high-resolution synchrotron X-ray and neutron diffraction is warranted. Here we report a systematic study of the crystal structures in the two series $BaLnSbO_6$ and Ba_2LnNbO_6 with particular attention being paid to the elucidation of both the nature of the phase transitions in these materials and determining if crystal chemistry can be used to explain the difference in symmetries adopted by these two series.

2. Experimental

All starting materials were obtained from Aldrich Chemicals. The lanthanide oxides and barium carbonate were dried prior to use by heating overnight at 1000 and 100 °C, respectively. Samples of Ba_2LnSbO_6 ($Ln = La^{3+}$, Pr^{3+}–Lu^{3+} and Y^{3+}) were prepared from stoichiometric mixtures of $BaCO_3$, Sb_2O_3 and, in the majority of cases, Ln_2O_3. In the cases of $Ln = Pr^{3+}$ and Tb^{3+} samples were made using Pr_6O_{11} and Tb_4O_7. The appropriate starting oxides were finely ground and then sequentially heated in air for periods of 24 h at 800, 1000, 1100, and 1200 °C. The samples were then heated for up to 48 h at 1300 °C with further heating at 1350 °C if required. Samples of Ba_2LnNbO_6 were prepared from the same starting materials substituting Nb_2O_5 for Sb_2O_3. These oxides were first pressed into pellets before heating at 1300 °C for 24 h at with subsequent heating at 1400 °C for successive periods of 24 h up to a maximum heating time of 120 h. In all cases samples were reground and, in the case of Ba_2LnNbO_6, repelleted after each stage of the heating process.

The reactions were monitored by powder X-ray diffraction using Cu-$K\alpha$ radiation on a Shimadzu X-6000 Diffractometer. Synchrotron X-ray diffraction data for the final samples were recorded on the Debye Scherrer diffractometer at the Australian National Beamline Facility, Beamline 20B at the Photon Factory, Tsukuba, Japan [14]. The samples were housed in 0.3 mm capillaries that were continuously rotated during measurement to reduce the effects of preferred orientation. Data were collected using three image plates as detectors covering the range of $5 < 2\theta < 125°$ with a step size of 0.01° and a wavelength of 0.82606 Å for measurements at ambient temperature and 0.80123 or 0.9999 Å for variable temperature measurements. Variable temperature measurements, at temperatures of up to 800 °C, were carried out using a custom built furnace over a range of $5 < 2\theta < 85°$. A diffraction pattern of Ba_2LaSbO_6 was collected on Beamline BL02B2 at SPring-8 at 100 K using X-rays of a wavelength of 0.7750 Å. The sample was cooled using a liquid N_2 cryostream.

Neutron powder diffraction data were collected for selected samples at room temperature using the high-resolution diffractometer, HRPD, at the HIFAR reactor operated by the Australian Nuclear Science and Technology Organization (ANSTO), Lucas Heights, Australia using a wavelength of either 1.4924 or 1.4928 Å over the angular range $10 < 2\theta < 150°$ with a step size of 0.05° [15]. The samples were held in 12 mm vanadium cans that were continuously rotated during the measurements. Neutron diffraction patterns of Ba_2NdNbO_6 above ambient temperature were obtained with the medium resolution neutron diffractometer (MRPD) at the same facility using a P 1100 furnace [16]. Data were collected at a wavelength of 1.665 Å from 5° to 138° (2θ angles) with a step size of 0.1°.

Refinements of the crystal structure were performed with the program RIETICA [17]. The diffraction peaks were described by a pseudo-Voight function using a Howard asymmetry correction where necessary [17]. For neutron diffraction patterns the background was calculated using a six-parameter polynomial while for the X-ray patterns the background was estimated from interpolation between up to 40 selected points.

3. Results and discussion

Establishing the correct symmetry and space groups for perovskite-type oxides can be far from trivial, relying on examination of both splitting of the strongest Bragg reflections to yield the cell metric and the systematic presence and/or absence of the weaker superlattice reflections due to cation ordering, octahedral tilting, cation displacement or a combination of these. In the present work, we have assigned space groups as those with the highest possible symmetry that accounts for all the observed reflections and is in-keeping with the group theoretical analysis of Howard, Kennedy and Woodward [15].

3.1. Ambient temperature structures

3.1.1. Niobates

Synchrotron X-ray diffraction patterns of the three oxides Ba_2LnNbO_6, Ln^{3+} = La, Pr, and Nd, show peak splitting indicative of monoclinic symmetry as previously reported [7] (see Fig. 1). The two most commonly observed monoclinic double perovskite structures are in $P2_1/n$ (tilt system $a^-a^-c^+$) and $I2/m$ (tilt system $a^-a^-c^0$). A neutron diffraction pattern of Ba_2NdNbO_6 features only R-point reflections, with no evidence of M- or X-point reflections found. This demonstrates that only out-of-phase tilting is present in this compound showing $I2/m$ to be appropriate space group. Similarly there was no indication of either M- or X-point reflections in the X-ray diffraction patterns of Ba_2LaNbO_6 or Ba_2PrNbO_6 suggesting they also adopt $I2/m$ symmetry. That the monoclinic compounds adopt $I2/m$ and not $P2_1/n$ symmetry is consistent with the previous report by Fu and IJdo [7] but not that of Hemi et al. [13], who reported that all members of this series of compounds adopt $P2_1/n$ symmetry. The refined structural parameters for Ba_2NdNbO_6 are listed in Table 1.

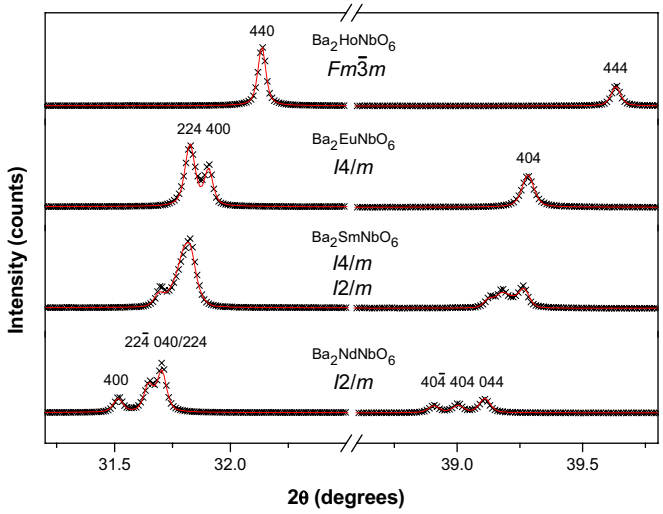

Fig. 1. Selected regions of X-ray diffraction patterns of Ba_2LnNbO_6 highlighting the differences in splitting of various peaks associated with different symmetries. In all cases the solid lines are the fits to the models described in the text.

The splittings of the Bragg reflections observed in the synchrotron X-ray diffraction patterns of the four Ba_2LnNbO_6 oxides with Ln = Eu–Dy were consistent with $I4/m$ tetragonal symmetry. A neutron diffraction pattern of Ba_2TbNbO_6 was also well fitted by a model using this symmetry. Attempts to fit the synchrotron X-ray diffraction pattern of Ba_2SmNbO_6 to structures in either monoclinic, $I2/m$, or tetragonal, $I4/m$, space groups were, however, unsuccessful. The observed profile was well fitted using a model that contained approximately equimolar amounts of these two phases ($R_p = 5.2$, $R_{wp} = 4.7\%$ for the two phase model cf. $R_p = 17.9$, $R_{wp} = 10.6\%$ in $I2/m$ and $R_p = 18.0$, $R_{wp} = 18.9\%$ in $I4/m$). The co-existence of these two phases most likely reflects that the temperature of the first-order transition between monoclinic and tetragonal symmetry for Ba_2SmNbO_6 is very close to room temperature. A X-ray diffraction pattern of Ba_2SmNbO_6 at 100 °C did not show any evidence for the presence of the monoclinic phase and was reasonably well fitted ($R_p = 5.6$, $R_{wp} = 7.6\%$) using a single phase tetragonal ($I4/m$) model confirming this suggestion. The remaining niobates; Ln = Ho–Lu and Y, are assigned as having $Fm\bar{3}m$ cubic symmetry, there being no obvious splitting of the Bragg reflections in their X-ray diffraction patterns. A neutron diffraction pattern of Ba_2ErNbO_6 was well fitted by this symmetry, Table 1. The lattice parameters of the 14 members of the series Ba_2LnNbO_6 are displayed in Fig. 2 illustrating the increase in symmetry of the structures as the size of the lanthanide ion gets smaller.

3.1.2. Antimonates

Synchrotron X-ray diffraction patterns of the oxides Ba_2LnSbO_6 with the largest lanthanides, La–Nd, showed well resolved splitting of the main Bragg reflections demonstrating the symmetry to be lower than cubic (see Fig. 3). The observed splitting pattern is indicative of rhombohedral symmetry. Neutron diffraction patterns obtained for both Ba_2PrSbO_6 and Ba_2NdSbO_6 contained only R-point superlattice reflections showing the structure contained only out-of-phase tilting of the BO_6 octahedra and it was concluded that the space group for these three oxides is $R\bar{3}$. The diffraction patterns for the antimonate compounds containing the smaller lanthanides (Sm^{3+}–Lu^{3+} and Y^{3+}) did not show any evidence for peak splitting with refinements in cubic space group $Fm\bar{3}m$ providing excellent fits to the X-ray diffraction patterns of these 11 samples. The transition from rhombohedral to

Table 1
Lattice parameters and atomic positions for selected members of $Ba_2LnB'O_6$ determined using neutron diffraction data

Compound	Ba_2NdNbO_6	Ba_2TbNbO_6	Ba_2ErNbO_6	Ba_2PrSbO_6	Ba_2NdSbO_6	Ba_2ErSbO_6
Space group	$I2/m$	$I4/m$	$Fm\bar{3}m$	$Fm\bar{3}m$	$R\bar{3}$	$Fm\bar{3}m$
a (Å)	6.0796(1)	5.9816(1)	8.4193(2)	6.0529(1)	6.0184(2)	8.3960(1)
b (Å)	6.0452(1)	$=a$	$=a$	$=a$	$=a$	$=a$
c (Å)	8.53823(2)	8.4757(2)	$=a$	$=a$	$=a$	$=a$
α (deg)	90	90	90	60.147(2)	60.077(3)	90
β (deg)	90.147(1)	90	90	$=\alpha$	$=\alpha$	90
γ (deg)	90	90	90	$=\alpha$	$=\alpha$	90
Ba	$4i$ (x,0,z)	$4d$ (0,1/2,1/4)	$8c$ (1/4,1/4,1/4)	$2c$ (x,x,x)	$2c$ (x,x,x)	$8c$ (1/4,1/4,1/4)
x	0.5030(5)	0	1/4	0.2505(4)	0.2564(4)	1/4
z	0.2482(5)	1/4	1/4	x	x	1/4
B (Å^2)	0.86(2)	0.96(2)	0.58(2)	0.72(3)	0.56(4)	0.67(2)
Ln	$2a$ (0,0,0)	$2a$ (0,0,0)	$4a$ (0,0,0)	$1a$ (0,0,0)	$1a$ (0,0,0)	$4a$ (0,0,0)
B (Å^2)	0.30(3)	0.62(5)	0.49(4)	0.56(7)	0.49(5)	0.52(4)
B'	$2d$ (0,0,1/2)	$2b$ (0,0,1/2)	$4b$ (1/2,1/2,1/2)	$1b$ (1/2,1/2,1/2)	$1b$ (1/2,1/2,1/2)	$4b$ (1/2,1/2,1/2)
B (Å^2)	0.35(3)	0.51(5)	0.29(4)	0.18(5)	0.39(7)	0.46(5)
O 1	$4i$ (x,0,z)	$4e$ (0,0,z)	$24e$ (x,0,0)	$6f$ (x,y,z)	$6f$ (x,y,z)	24e (x,0,0)
x	0.0512(3)	0	0.2639(1)	0.7310(4)	0.7221(6)	0.2638(1)
y	0	0	0	0.2390(3)	0.2360(4)	0
z	0.2686(3)	0.2665(5)	0	0.2988(2)	0.2927(4)	0
B (Å^2)	1.19(4)	1.26(8)	1.01(2)	1.13(2)	1.69(3)	0.92(2)
O 2	$8j$ (x,y,z)	$8h$ (x,y,0)				
x	0.2694(3)	0.2441(4)				
y	0.2665(4)	0.2821(4)				
z	0.9729(2)	0				
B (Å^2)	1.40(3)	1.45(4)				
R_p (%)	4.1	5.5	5.9	6.2	5.2	6.0
R_{wp} (%)	4.9	6.5	7.2	7.3	7.3	7.2
χ^2 (%)	2.0	2.5	1.7	1.5	1.5	1.9

cubic symmetry occurs between Nd^{3+} and Sm^{3+} corresponding to lanthanide ionic radii of between 0.96 and 0.98 Å. These results are consistent with previous work by Fu and IJdo [6]. Fig. 2 presents the lattice parameters of this series as determined by synchrotron X-ray diffraction. It should be noted that the possibility of anti-site disorder of the two B-type cations was investigated for all the compounds studied. Without exception the refinements indicated complete ordering of the B-type cations over the two sites. This is as expected due to the large size difference between the lanthanide and Nb^{5+} and Sb^{5+} cations [18].

3.1.3. Bond valence

Atomic positions and bond distances for selected members of the antimonate and niobate series, as determined by neutron diffraction, are recorded in Tables 1 and 2, respectively. In all cases the bond valence sums (BVS) of the Ba^{2+} cations are significantly less then 2.0 demonstrating that the average Ba–O bond distances are longer than optimal. As previously noted when the size of the lanthanide ion decreases the Ba–O bond distances decreases resulting in the bond valency of the Ba^{2+} site getting closer to the ideal value of two [6,7,19]. This increased bond valency reflects that the size of the A-site is becoming more suitable for the Ba^{2+} cation reducing the requirement for octahedral tilting in the structure and therefore resulting in higher symmetry.

A feature of the oxides described here is the large size difference between the two B-type cations, the M^{5+} cations being very much smaller than the Ln^{3+} cations. The bond lengths and BVS provide further insight into the bonding required when two significantly different sized ions are distributed over the two B-sites of an ordered double perovskite structure. In both series the Ln^{3+} ions are consistently overbonded with the Ln–O bond lengths being significantly shorter than what would be expected based on their ionic radii [18]. This is clearly illustrated by the average BVS of the lanthanides being 3.49 in the antimonates and 3.38 for the niobates. On the other hand the mean Sb–O bond lengths of 1.98(2) Å are close to the value expected from ionic radii (2.00 Å) giving band valence sums in good agreement with the formal valence of the Sb^{5+} cation. The mean Nb–O bond lengths (1.99(2) Å) are, however, significantly shorter than the expected 2.04 Å [18] and this is expected to give higher than expected BVS. To our surprise the BVS for the Nb^{5+} cations are systematically less than 5.0. This may reflect an

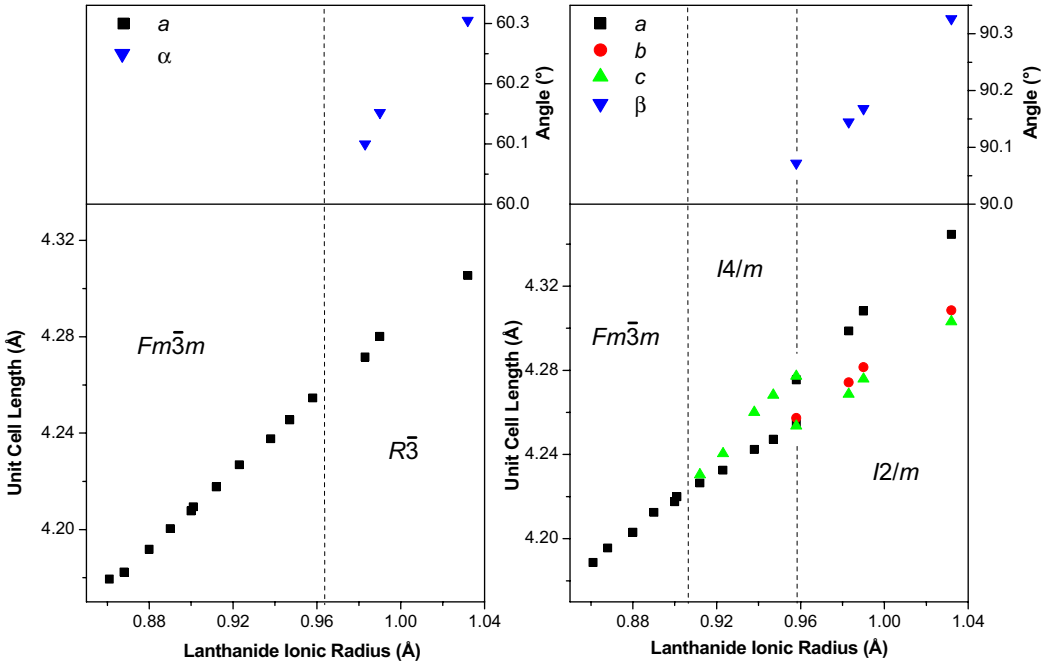

Fig. 2. Reduced lattice parameters of members of the series Ba_2LnSbO_6 (left) and Ba_2LnNbO_6 (right) at ambient temperature indicating the increased deviation from the metrically cubic structure as the size of the lanthanide ion increases.

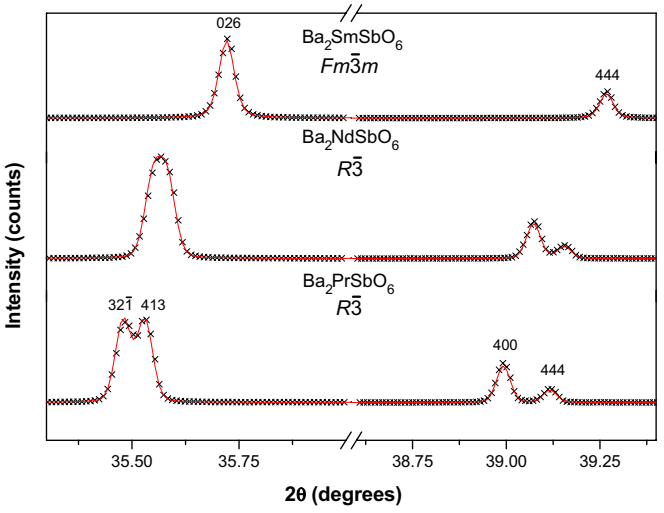

Fig. 3. Selected regions of synchrotron X-ray diffraction patterns of Ba_2LnSbO_6 highlighting the differences in splitting of various peaks associated with different symmetries.

error in the bond valence parameter r_o as determined by Brown and Altermatt used to determine the bond valencies of ions in these compounds [19], although a more recent study by Brese and O'Keeffe found a comparable value for r_o suggesting that this is not likely to be the case [20]. It is possible that the ionic radii of Nb^{5+} does not accurately reflect its size in this co-ordination environment.

The overbonding of the lanthanide cations is most likely a consequence of having the large lanthanides on the perovskite B-sites. The suitability of any cation pair to form a perovskite-type structure is generally expressed in terms of the tolerance factor, which essentially predicts that as the size of the B-type cation increases the A–O bond distance must also increase, unless there is a significant structural distortion. In the present case the Ba–O bond distances are longer than optimal (bond valences significantly less than 2.0) and it appears that there is a compromise between the bonding requirements of the A- and B-site cations resulting in the underbonding of the Ba^{2+} ions and overbonding of the Ln^{3+} ions. In tilted structures a combination of expanding the size of *Ln*–O bonds while maintaining the same unit cell size, and hence bonding environment of the Ba^{2+} cations, could be achieved by increasing the tilting of the octahedra. This could potentially provide a means to further optimize the bonding conditions for all cations. That this does not occur implies that there are other competing factors favoring smaller rotation of the octahedra. Unlike the Sb–O bond lengths the Nb–O bond lengths are smaller than expected. This is most likely a consequence of the *Ln*–O bonds being as short as is chemically reasonable in the antimonate series. Thus these bonds cannot contract further when the larger Nb^{5+} ion ($r = 0.64$ Å) substitutes for Sb^{5+} ($r = 0.60$ Å). This results in the average *B*′–O bond lengths being similar in the antimonate and niobate series, despite the bonding problems suggested by the BVS calculations. That these oxides form perovskites, despite the severe bonding problems revealed by the bond valence calculations, is testament to the renowned compositional flexibility of perovskites.

Table 2
Bond lengths and bond valence sums (BVS) for selected members of $Ba_2LnB'O_6$ determined using neutron diffraction data

Compound	Ba–O		Ln–O		B′–O	
	Average bond length (Å)	BVS	Bond length (Å)	BVS	Bond length (Å)	BVS
Ba_2NdNbO_6	$12 \times 3.037(1)$	1.80	$2 \times 2.314(3)$ $4 \times 2.309(2)$	3.44	$2 \times 2.001(3)$ $4 \times 2.002(4)$	4.69
Ba_2TbNbO_6	$12 \times 2.996(1)$	1.84	$2 \times 2.259(4)$ $4 \times 2.231(3)$	3.57	$2 \times 1.979(4)$ $4 \times 2.011(3)$	4.72
Ba_2ErNbO_6	$12 \times 2.9790(1)$	1.86	$6 \times 2.222(1)$	3.39	$6 \times 1.988(1)$	4.87
Ba_2PrSbO_6	$12 \times 3.037(1)$	1.69	$6 \times 2.312(2)$	3.72	$6 \times 1.989(2)$	5.29
Ba_2NdSbO_6	$12 \times 3.017(1)$	1.85	$6 \times 2.259(2)$	4.09	$6 \times 2.016(3)$	4.92
Ba_2ErSbO_6	$12 \times 2.9707(1)$	1.91	$6 \times 2.215(1)$	3.45	$6 \times 1.983(1)$	5.37

3.2. Variable temperature studies

3.2.1. Niobates

The nature of the phase transitions of representative examples of the Ba_2LnNbO_6 and Ba_2LnSbO_6 series have been studied, for the first time, using variable temperature synchrotron X-ray diffraction. As shown in Fig. 4, Ba_2NdNbO_6 undergoes a first-order phase transition between $I2/m$ and $I4/m$ symmetry, with these two phases co-existing between 235 and 355 °C. The co-existence of these two phases indicates that the phase transition is first order in nature in accordance with Landau theory as determined as part of the group theoretical analysis of double perovskites carried out by Howard et al. [21]. The kinetics of the transition between the two phases is unknown however it is likely that the temperature range over which the two phases co-exist will depend on the heating rate. The time taken to collect the data in the two-phase region was approximately 2 h, suggesting that the temperature range found over which these two phases co-exist reflects the relative thermodynamic stability of the two phases. The existence of a first-order phase transition has implications for applications involving members of this series that are monoclinic at room temperature. A first-order phase transition could result in delaminating and cracking of devices in which these materials are used due to small discontinuities in the volume between the two phases.

Above 425 °C the structure of Ba_2NdNbO_6 was found to be cubic and the structure was refined in space group $Fm\bar{3}m$ (see Fig. 4). The $I4/m$ to $Fm\bar{3}m$ phase transition appears to be continuous. An analysis of the spontaneous strain of the tetragonal phase (e_t) was carried out in order to further discern the nature of this transition. For this transition the spontaneous strain is proportional to the order parameter (Q) squared and can be estimated as [22]

$$e_t = \frac{2}{\sqrt{3}}\left(\frac{c - a\sqrt{2}}{a_0}\right),$$

where c and a are the lattice parameters of the tetragonal phase and a_0 is the estimated value of the lattice parameter of the cubic structure assuming no phase transition had taken place. A plot of e_t^2 versus temperature was linear suggesting that the phase transition is continuous and tricritical in nature (see Fig. 5). Extrapolation of the spontaneous strain to zero indicates that the phase transition should occur at 422(2) °C, well within the temperature range of 415–425 °C determined experimentally, from the appearance of the diagnostic peak splitting observed in the X-ray diffraction patterns.

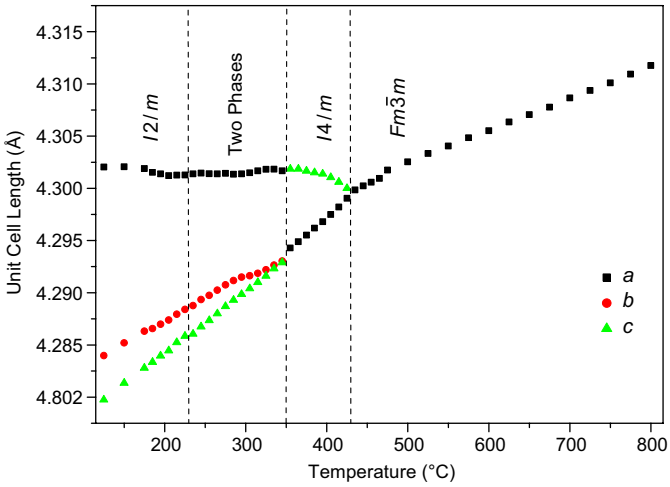

Fig. 4. Temperature dependence of the reduced lattice parameters for Ba_2NdNbO_6 obtained from analysis of synchrotron X-ray diffraction data. For clarity only the parameters for the monoclinic phase are shown in the two-phase region.

The structure of Ba_2NdNbO_6 was also investigated at small number of temperatures using medium resolution neutron diffraction data. Such data were used to accurately determine the angle of the out-of-phase tilts, ϕ, of the BO_6 octahedra. This tilt angle serves as another measure of distortion in the structure and was found to be 7.8° at room temperature and decreased slightly to 6.9° at 200 °C. Interestingly ϕ was found to be 5.2° for the tetragonal phase at 400 °C before decreasing rapidly to zero above 425 °C as required by cubic symmetry. This suggests that the octahedral tilt angle is not significantly affected by the discontinuous phase transition between monoclinic and tetragonal symmetry [23,24].

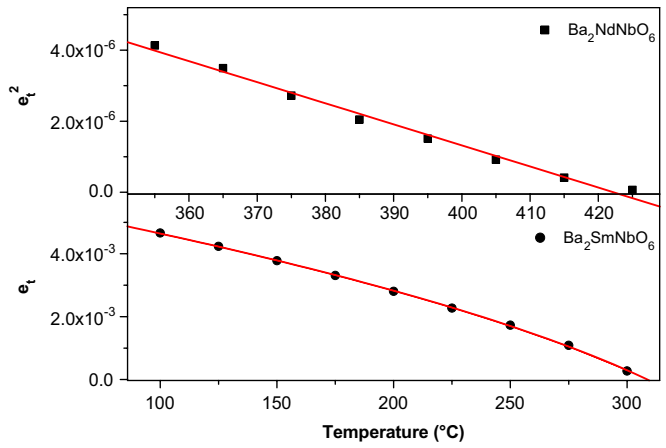

Fig. 5. Temperature dependence of square of tetragonal strain for Ba_2NdNbO_6 and the tetragonal strain versus temperature for Ba_2SmNbO_6 highlighting the presence of the higher-order terms in the Landau theory. The fit to tetragonal temperature versus strain for Ba_2SmNbO_6 is in the form $e_t = \sqrt{1 + k(T_c - T)} - 1$.

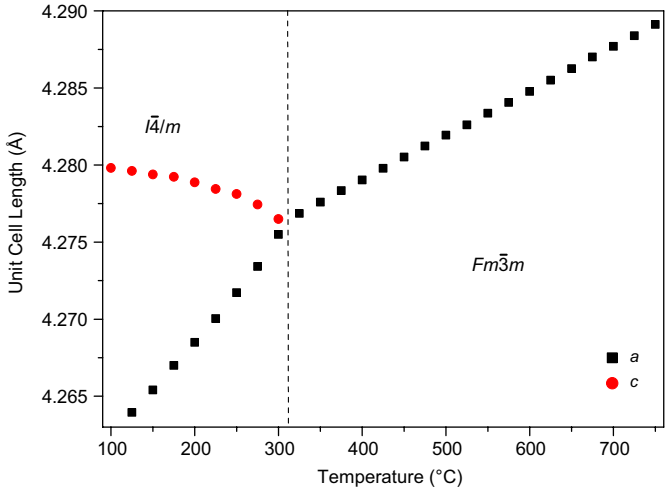

Fig. 6. Temperature dependence of the reduced lattice parameters for Ba_2SmNbO_6 obtained from analysis of synchrotron X-ray diffraction data.

As noted above Ba_2SmNbO_6 undergoes a first-order $I2/m$ to $I4/m$ transition near room temperature. X-ray diffraction measurements at higher temperatures indicate that this undergoes a continuous phase transition from tetragonal to cubic symmetry near 300 °C (see Fig. 6). A fit of spontaneous strain in the tetragonal structure versus temperature is approximately linear. A better fit is, however, obtained by adding a quadratic term to this fit (see Fig. 5). This is attributed to a contribution from the Q^6 term in the Landau free energy expansion. As is expected in this case a plot of spontaneous strain versus $\sqrt{1 + k(T_c - T)} - 1$, was linear with $T_c = 309(1)$ °C and $k = 0.018(2)$ [25]. It is unclear why the contribution from higher-order terms in the Landau free energy expansion are more significant for Ba_2NdNbO_6 than for Ba_2SmNbO_6. In both cases the presence of these higher-order terms shows that the phase transition is not second order and suggests the presence of an additional instability. The spontaneous strain analysis indicates that the phase transition occurs at approximately 309 °C, well within the range determined by the loss of the diagnostic splitting monitored by X-ray diffraction.

3.2.2. Antimonates

The structure of Ba_2LaSbO_6 was studied over the range of 100–520 °C with a phase transition between rhombohedral $R\bar{3}$ and cubic $Fm\bar{3}m$ symmetry being found to occur above 400 °C (see Fig. 7). A plot of α versus temperature was linear suggesting that this phase transition is second order in nature. This is consistent with group-theoretical analysis previously carried out by Howard et al. [21]. The spontaneous strain due to the rhombohedral distortion is proportional to the difference of the rhombohedral angle from $\pi/3$ [23] and the temperature dependence of this is shown in Fig. 7. An extrapolation of this plot to zero strain suggests, that the phase transition occurs at 438(2) °C. The difference between the temperature of the phase transition estimated by extrapolation and the temperature at which the diagnostic peak splitting is no longer experimentally observed highlights the shortcomings of estimating phase transitions using peak splitting where the instrument resolution is insufficient to separate very small splitting of peaks.

The synchrotron X-ray diffraction pattern of Ba_2LaSbO_6 at 100 K indicated splitting consistent with monoclinic symmetry (see Fig. 8). There was no indication of M- or X-point reflections in the pattern indicating that the structure adopts $I2/m$ symmetry. This is significant as it demonstrates that the compounds in the series Ba_2LnSbO_6 adopt the same monoclinic symmetry as those in the Ba_2LnNbO_6 series. This highlights that the only difference in phases adopted by the two series appear to be the preference for the antimonates to adopt rhombohedral symmetry while the niobates adopt tetragonal symmetry, a point we shall return to.

That the rhombohedral to cubic phase transition in Ba_2LaSbO_6 is second order but the tetragonal to cubic phase transition in the niobates feature contributions from higher-order terms of the Landau free energy expression is worth noting. As previously mentioned the presence of another term in the Landau free energy expansion indicates the presence of an additional instability. This may reflect the presence of a third nearby phase. This phase may well be a rhombohedral structure analogous to that adopted by the antimonate series. If this postulate is correct then it appears that the energy difference between the rhombodedral and tetragonal phases is relatively small in these systems.

3.2.3. Similar but different

In their work, Fu and IJdo [7] suggested that the higher electronegativity of Sb^{5+} compared to Nb^{5+} results in an increase in the covalency of the bonding in the antimonate series, as well as in the analogous Ba_2LnBiO_6, Ba_2LnRuO_6

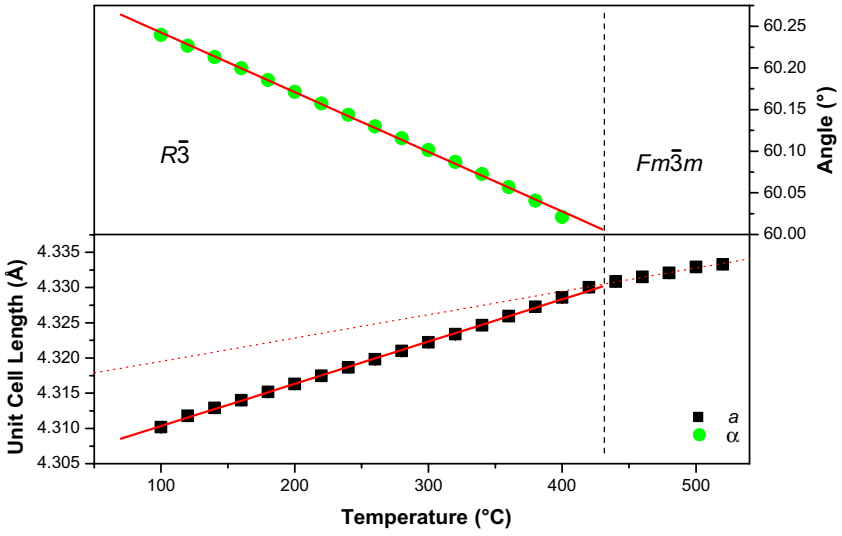

Fig. 7. Temperature dependence of the reduced lattice parameters for Ba_2LaSbO_6 obtained from analysis of synchrotron X-ray diffraction data.

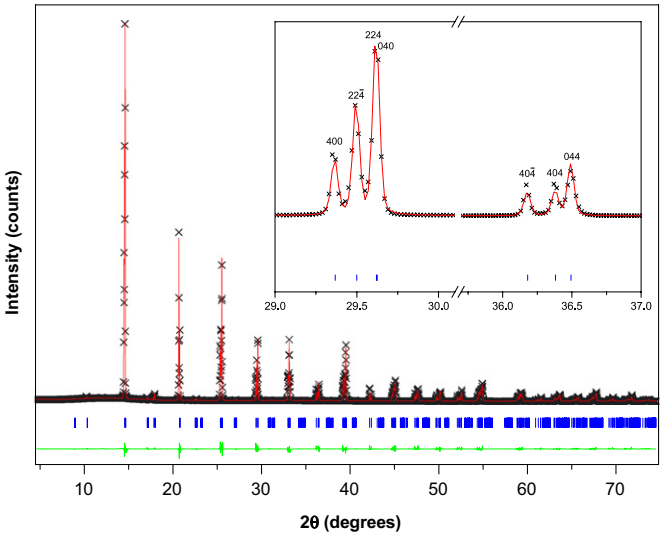

Fig. 8. Synchrotron X-ray diffraction pattern of Ba_2LaSbO_6 at 100 K. The crosses, continuous line and lower continuous line represent the observed pattern, the calculated pattern and difference plot respectively. The vertical lines are the Bragg reflection markers. The insert highlights the splitting in the diffraction pattern indicative of monoclinic symmetry with the corresponding peaks in the full diffraction pattern being indicated by arrows.

and Ba_2LnIrO_6 compounds [6–10]. This results in these oxides adopting rhombohedral symmetry whereas the corresponding Ba_2LnNbO_6 oxides adopt tetragonal symmetry. However, no reason for this preference of rhombohedral symmetry for those series containing high degrees of covalent bonding was given. The recent report [11] that Ba_2NdMoO_6 has tetragonal symmetry at ambient temperature, creates further uncertainty since Mo^{5+} has comparable electronegativity to those B' ions in series which adopt rhombohedral symmetry [12]. This is particularly significant in the case where $B' = Bi^{5+}$ and Sb^{5+} which adopt rhombohedral symmetry despite having electronegativities between Nb^{5+} and Mo^{5+} both of which adopt tetragonal symmetry [26]. This leads us to question whether electronegativity alone is the cause of this difference in symmetry. Simple size arrangements also appears unlikely to be the cause of this difference in symmetry as Nb^{5+} and Mo^{5+} have ionic radii intermediate of those of Sb^{5+} and Bi^{5+}. It is possible that a second-order Jahn-Teller (SOJT) effect, that may be active in the NbO_6 octahedra but not in the SbO_6 octahedra due to the former having a d^0 electronic configuration, could explain the difference in the phase transitions of the two series. There is, however, no indication of a significant difference between the six niobium-oxygen bond lengths in either the monoclinic or tetragonal niobates; see Table 2 as would be expected for a structure exhibiting a SOJT effect. Thus any SOJT effect, if present, must be weak and we do not believe this will be responsible for the difference between the two symmetries.

It is therefore most likely that the difference in symmetry between the Ba_2LnNbO_6 and Ba_2LnSbO_6 oxides is due to, a subtle, electronic effect. The most significant difference between Sb^{5+} and Nb^{5+} is that Nb^{5+} has empty 4*d* orbitals while Sb^{5+} has a full 4*d* shell. This means that the 4*d* orbitals of the niobium ions in Ba_2NdNbO_6 are available to take part in π-bonding with the oxygen anions whereas the Sb 4*d* orbitals cannot. Woodward [27] has suggested that when there is significant π-bonding between the B-site cations and the oxygen anions and if the metal has only a few electrons in its *d*-orbitals, the perovskite structure with M–O–M angles closest to 180° will be favoured.

The pair of oxides, Ba_2NdNbO_6 and Ba_2NdSbO_6, provides a convenient test of Woodward's hypothesis. The former is tetragonal in $I4/m$ at 400 °C and later rhombohedral at room temperature. Both undergo a continuous transition to a cubic structure on heating. All the Nd–O–Sb bond angles in Ba_2NdSbO_6 are 169.8(1)°

whereas the Nd–O–Nb bonds angles in Ba_2NdNbO_6 are divided into two types. The first, involving O1 on the 4*e* site, has a Nd–O1–Nb bond angle of 180° as required by the symmetry of the structure. The second involving O2, the oxygen occupying the 8*h* site, has a Nd–O2–Nb bond angle of 169.6(4)°. While there are twice as many Nd–O2–Nb bonds as there are Nd–O1–Nb bonds, critically one-third of the Nd–O–Nb bonds are 180° in the tetragonal structure compared to none in the rhombohedral structure. The other bond angles are similar in size in the two structures. This difference appears to be sufficient to stabilize the tetragonal structure. Of course the impact of this difference in bonding will only be evident in systems with similar tolerance factors and electrostatic (valence) arrangements. Although niobium is nominally pentavalent in these oxides and therefore has no electron density in its 4*d* orbitals if these oxides posses significant covalent bonding character rather than the bonding being completely ionic, the niobium ions would maintain some electron density in their 4*d* orbitals.

The above explanation also accounts for the observed structures in other $Ba_2LnB'O_6$ series. Mo^{5+} in tetragonal Ba_2NdMoO_6 has one *d*-electron while the series known to adopt rhombohedral symmetry contain *B*′ ions with more *d*-electrons, Ru^{5+}, Ir^{5+}, and Bi^{5+} have d^3, d^4, and d^{10} configurations, respectively. This suggests that the transition between series which adopt tetragonal symmetry and those that adopt rhombohedral symmetry is between d^1 and d^3 configurations. Examination of other $Ba_2LnB'O_6$ series which have electronic configuration between d^1 and d^3 is warranted to provide further insight into the relative stability of tetragonal and rhombohedral phases in similar series.

4. Conclusion

The structures of 28 members from the two series Ba_2LnNbO_6 and Ba_2LnSbO_6 have been examined using neutron and synchrotron X-ray diffraction. It has been found that at room temperature the former displays the series of phases $I2/m$ to $I4/m$ to $Fm\bar{3}m$ depending on the size of the Ln^{3+} cation while the latter series adopts rhombohedral $R\bar{3}$ symmetry in preference to the tetragonal $I4/m$ phase. Variable temperature X-ray diffraction indicates that the phase transition from monoclinic to tetragonal symmetry in the niobates is first order and discontinuous while the phase transitions between tetragonal and cubic symmetry and rhombohedral and cubic symmetry are continuous. It is suggested that π-bonding is the cause of the niobates adopting tetragonal symmetry in preference to rhombohedral symmetry adopted by the antimonates. Finally persistent overbonding of the lanthanide cations has been found providing an indication of the structural compromise required in a perovskite structure containing unusually large B-site cations.

Acknowledgments

This work has been partially supported by the Australian Research Council. The neutron diffraction work has been supported by the Australian Institute of Nuclear Science and Engineering (AINSE) through the provision of an AINSE Postgraduate Award. The work performed at the Australian National Beamline Facility was supported by the Australian Synchrotron Research Program under the Major National Research Facilities program and was performed with the help of Dr. James Hester. The authors would also like to thank Dr. Chris Howard for collecting the low-temperature synchrotron X-ray diffraction pattern of Ba_2LaSbO_6 at SPring-8.

References

[1] J. Kurian, A.M. John, P.K. Sajith, J. Koshy, S.P. Pai, R. Pinto, Mater. Lett. 34 (1998) 208–212.
[2] J. Kurian, J. Koshy, P.R.S. Wariar, Y.P. Yadava, A.D. Damodaran, J. Solid State Chem. 116 (1995) 193–198.
[3] P. Murugaraj, K.D. Kreuer, T. He, T. Schober, J. Maier, Solid State Ion. 98 (1997) 1–6.
[4] P.J. Saines, M.M. Elcombe, B.J. Kennedy, Physica B, in press.
[5] R.H. Mitchell, Perovskites Modern and Ancient, Almaz Press Inc., Ontario, 2002.
[6] W.T. Fu, D.J.W. IJdo, J. Solid State Chem. 178 (2005) 2363–2367.
[7] W.T. Fu, D.J.W. IJdo, J. Solid State Chem. 179 (2006) 1022–1028.
[8] W.T.A. Harrison, K.P. Reis, A.J. Jacobson, L.F. Schneemeyer, J.V. Waszczak, Chem. Mater. 7 (1995) 2161–2167.
[9] W.T. Fu, D.J.W. IJdo, Solid State Commun. 136 (2005) 456–461.
[10] W.T. Fu, D.J.W. IJdo, J. Alloys Compd. 394 (2005) L5–L8.
[11] E.J. Cussen, D.R. Lynham, J. Rogers, Chem. Mater. 18 (2006) 2855–2866.
[12] L. Pauling, The Nature of the Chemical Bond and the Structure of Molecules and Crystals: An Introduction to Modern Structural Chemistry, Cornell University Press, Ithaca, 1960.
[13] K. Henmi, Y. Hinatsu, N.M. Masaki, J. Solid State Chem. 148 (1999) 353–360.
[14] T.M. Sabine, B.J. Kennedy, R.F. Garrett, G.J. Foran, D.J. Cookson, J. Appl. Crystallogr. 28 (1995) 513–517.
[15] C.J. Howard, C.J. Ball, R.L. Davis, M.M. Elcombe, Aust. J. Phys. 36 (1983) 507–518.
[16] S.J. Kennedy, Adv. X-Ray Anal. 38 (1995) 35–46.
[17] B.A. Hunter, C.J. Howard, A Computer Program for Rietveld Analysis of X-Ray and Neutron Powder Diffraction Patterns, Lucas Heights Laboratories, 1998.
[18] R.D. Shannon, Acta Crystallogr. A 32 (1976) 751–767.
[19] I.D. Brown, D. Altermatt, Acta Crystallogr. B 41 (1985) 244–247.
[20] N.E. Brese, M. O'Keeffe, Acta Crystallogr. B 47 (1991) 192–197.
[21] C.J. Howard, B.J. Kennedy, P.M. Woodward, Acta Crystallogr. B 59 (2003) 463–471.
[22] M.A. Carpenter, in: S.A.T. Redfern, M.A. Carpenter (Eds.), Transformation Processes in Minerals, The Mineralogical Society of America, Washington, DC, 2000, pp. 35–64.
[23] B.J. Kennedy, C.J. Howard, K.S. Knight, Z. Zhang, Q. Zhou, Acta Crystallogr. B 62 (2006) 537–546.
[24] M.A. Carpenter, C.J. Howard, B.J. Kennedy, K.S. Knight, Phys. Rev. B 72 (2005) 024118/024111–024115.
[25] T.B. Ballaran, R.J. Angel, M.A. Carpenter, Eur. J. Mineral. 12 (2000) 1195–1213.
[26] K. Li, D. Xue, J. Phys. Chem. A 110 (2006) 11332–11337.
[27] P.M. Woodward, Acta Crystallogr. B 53 (1997) 44–66.